All-optical measurement of nuclear-spin relaxation

Robert Klieber, Andreas Michalowski, Rudolf Neuhaus,* and Dieter Suter
Universität Dortmund, Fachbereich Physik, 44221 Dortmund, Germany
(Received 22 April 2003; published 26 August 2003)

Nuclear-spin relaxation rates are usually measured by pulsed radio frequency excitation of nuclear-spin transitions. When the number of spins is too small for direct detection with conventional nuclear-magnetic-resonance spectrometers, pulsed excitation may be combined with optical detection of the nuclear spins for increased sensitivity. Here we demonstrate that such measurements can also be done purely optically, without radio frequency fields. This is achieved by preparing nonthermal populations by optical hole-burning and time-resolved probing of the populations as a function of the decay time. Measurements of the nuclear-spin relaxation of ^{141}Pr in the electronic ground state of Pr^{3+}:$YAlO_3$ show that the relaxation rates for the three transitions differ by a factor of 3.

DOI: 10.1103/PhysRevB.68.054426 PACS number(s): 39.30.+w, 76.60.−k

I. INTRODUCTION

When an intense narrow-band laser interacts with an ion or molecule with multiple nondegenerate ground states, it generally creates a nonthermal distribution of the populations of these states. In an inhomogeneously broadened ensemble, the redistributed populations can be probed with a second, independently tunable laser beam. At frequencies where this probe laser interacts with states whose populations have been reduced by the pump laser, its absorption is reduced. This occurs, e.g., when the probe laser is at the same frequency as the pump laser. The reduced absorption is referred to as a spectral hole and the resulting spectrum of the probe-laser beam is called a hole-burning spectrum.[1,2] Besides the holes, a hole-burning spectrum contains regions of increased absorption, where the probe laser interacts with levels whose populations are higher than in thermal equilibrium. These features are called antiholes.

The width of holes and antiholes can reach the homogeneous widths of the optical transitions even in strongly inhomogeneously broadened ensembles. Since the separation between holes and antiholes corresponds to differences between energy levels of the atom or molecule being probed, hole-burning spectra can be used to measure energies of atomic ground states with high resolution. This technique has been applied to the measurement of, e.g., low-temperature molecular dynamics[3] or of nuclear quadrupole coupling constants in electronic ground states as well as in excited states.[4–7]

Nuclear-spin relaxation processes are typically studied by nuclear-magnetic-resonance spectroscopy (NMR) or nuclear quadrupole resonance. In samples with small numbers of spins, the low sensitivity of NMR compared to other spectroscopic techniques often does not allow measurements with conventional NMR spectrometers. Optical techniques can sometimes be used to circumvent this problem. In particular, double-resonance techniques have been used.[8–12]

The different transitions of spins with $I>1$ usually decay with different rates. Depending on the detection scheme being used in an experiment, one often measures a linear combination of multiexponential decays, which makes it hard to extract individual rate constants, which can be analyzed in terms of elementary relaxation processes. One approach to obtain individual relaxation rates is to short circuit at least one of the rates by resonantly irradiating the corresponding transition with a radio frequency field.[11,13,14] However, the modification of the dynamics by the external field is nontrivial and it may lead to unwanted effects, such as heating of the sample by the applied rf field.

In this paper we present an alternate method for measuring the nuclear-spin relaxation rates, which does not involve rf irradiation. It uses a stabilized laser, whose frequency jitter is comparable to the homogeneous optical linewidth and significantly smaller than the quadrupole coupling constants. Hole-burning spectra with this laser resolve all possible optical transitions between the ground and excited states, allowing one to independently measure all spin populations in the electronic ground state. Time-resolved measurements of the decay of these populations can be fitted with the theoretical time dependence to obtain individual relaxation rates.

The paper is structured as follows. In Sec. II, we summarize the principles of hole-burning spectroscopy and the relaxation dynamics of the nuclear-spin system. Section III summarizes the experimental setup. The experimental results presented in Sec. IV allow us to measure the spin-relaxation rates in the electronic ground state of the rare-earth ion Pr in Pr^{3+}:$YAlO_3$. The paper concludes with a summary of the main results.

II. THEORY

A. Energy levels

The Pr^{3+} ions substitute Y ions in the $YAlO_3$ lattice. The low site symmetry (C_{1h}) leads to a quenching of the angular momentum and completely lifts the degeneracy of the electronic states. The nuclear-spin state degeneracy of ^{141}Pr is partly lifted in zero field by an effective quadrupole interaction.[15,16] As shown in Fig. 1, each electronic state splits therefore into three sets of double degenerate hyperfine states that can be labeled (approximately) with the nuclear-spin quantum numbers $m_I=\pm\frac{1}{2}$, $\pm\frac{3}{2}$, and $\pm\frac{5}{2}$.

The coupling constant varies with the electronic state; the resulting splittings are 7.1, 14.1, and 21.2 MHz in the $^3H_4$ electronic ground state and 0.9, 1.6, and 2.5 MHz in the

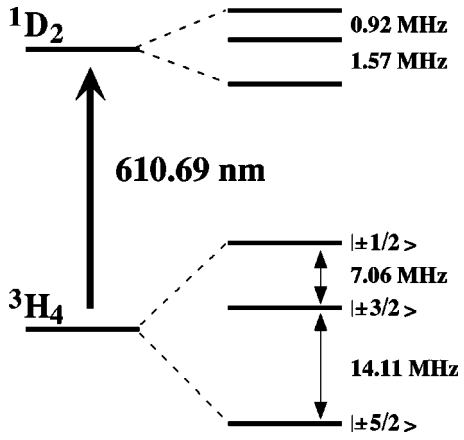

FIG. 1. Relevant part of the energy-level scheme of Pr^{3+}:$YAlO_3$. Each electronic state consists of three doubly degenerate nuclear-spin substates.

electronically excited $^1D_2$ state. Since all optical transitions between levels of the same $4f^N$ configuration are weakly allowed,[17] nine optical transitions are possible. The long lifetime of the excited state ($T_1 = 180\ \mu s$)[18,19] leads to a narrow homogeneous optical linewidth of approximately 10 kHz at low temperatures.

B. Hole-burning spectra

Since the linewidth of the laser ($\sim$20 kHz) is small compared to the separation between the hyperfine levels, it interacts at most with one optical transition of each ion. For those ions that are resonant, the laser redistributes the population from the resonant hyperfine state to the nonresonant states.

A probe-laser beam, whose frequency is scanned over a frequency range that includes the pump-laser frequency, monitors the changes of the ground-state populations: If the populations of the resonant states have been reduced by the pump laser, the absorption of the probe laser decreases and vice versa.[1] The spectral positions of reduced absorptions are referred to as spectral holes and the positions of increased absorption as antiholes.

Since the inhomogeneous width of the optical transitions (5 GHz in our crystal) is much larger than the ground-state splittings, the pump laser interacts with all of the nine possible transitions for some set of ions. Since the probe laser also can interact with each of these transitions, one can distinguish 81 different pump-probe combinations, which result in 49 distinct resonance line positions in the hole-burning spectrum.[7]

Figure 2 represents the resulting hole-burning spectrum. The upper trace shows the experimental spectrum, while the stick spectra below indicate the resonance line positions for the main pump configurations displayed schematically on the left. In each subspectrum, the leftmost group of lines measures the population of the $m_I = \pm\frac{1}{2}$ state, the second group [around -14 MHz in Fig. 2(a)] the population of $m_I = \pm\frac{3}{2}$ state, and the group at the highest frequency the $m_I = \pm\frac{5}{2}$ state. The seven lines correspond to different excited-state sublevels to which pump and probe lasers couple. The different amplitudes of the lines (see experimental trace) are due to different populations depending on the transition to which the pump laser couples as well as to different transition strengths of the probe transitions.

While some of the resonance lines represent the population change of a single nuclear-spin state of the electronic ground state, others are weighted averages of all ground states. Obviously, monitoring the nuclear-spin populations by optical spectroscopy is only possible if the frequency resolution of the laser is significantly better than the energy separation between the nuclear-spin states. In this system, the smallest splittings are in the electronically excited state.

If the pump-laser field is switched off, the modified nuclear-spin population relaxes towards thermal equilibrium, corresponding to equal populations in all ground states. The hole-burning spectrum provides a possible way of monitoring this decay: Fig. 3 shows several spectra obtained for increasing time delays between the pump- and a probe-laser pulses. The decay of the resonance lines with the delay clearly shows how the nuclear-spin system returns to thermal equilibrium.

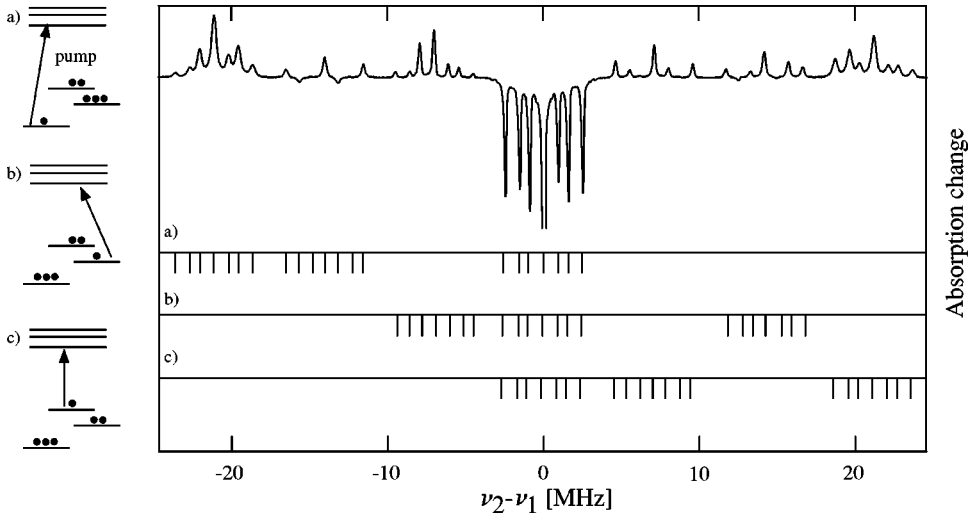

FIG. 2. The upper trace shows the experimental hole-burning spectrum of the 610.69-nm transition at 3 K as a function of the frequency difference $\nu_2 - \nu_1$ between the probe- and the pump-laser frequencies. The level schemes on the left-hand side show three pump configurations, and the stick spectra in the lower part of the figure represent the corresponding partial hole-burning spectra. For clarity the main hole at $\nu_2 = \nu_1$ has been truncated in the experimental spectrum.

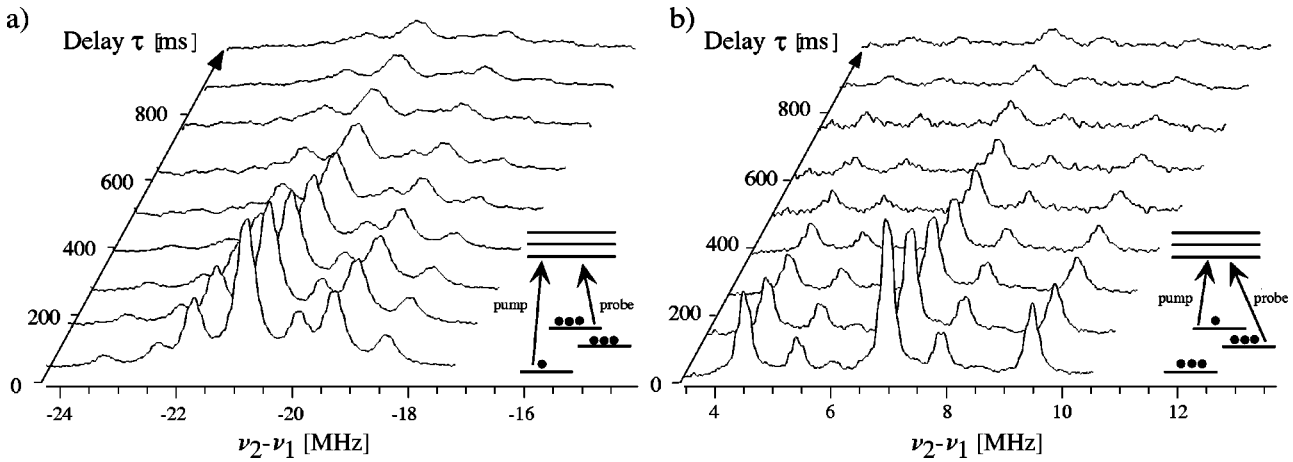

FIG. 3. Hole-burning spectra for the antiholes around (a) -21.2 MHz and (b) $+7.1$ MHz for different time delays τ between the pump- and the probe-laser pulses. As the delay between pump and probe pulses is increased, the nuclear-spin state populations approach their equilibrium values and the hole spectrum decays. The insets indicate the relevant energy scheme and the optical transitions to which the pump and the probe beams couple.

C. Nuclear-spin relaxation

To calculate the time dependence of the nuclear-spin populations after the end of the pump pulse, we only have to consider the ground-state sublevels; the excited-state populations are small and decay rapidly at the end of the pump pulse. We consider three ground states, which are doubly degenerate. Since the energy separation between the nuclear-spin substates is small compared to the thermal excitation energy $k_B T$, we assume that the equilibrium populations are equal and the relaxation rates are symmetric, $\Gamma_{ij}=\Gamma_{ji}; i,j=1,\ldots,3$. The relevant equation of motion is then

$$\frac{d}{dt}\begin{pmatrix} p_1 \\ p_2 \\ p_3 \end{pmatrix} = \begin{pmatrix} -(\Gamma_{12}+\Gamma_{13}) & \Gamma_{12} & \Gamma_{13} \\ \Gamma_{12} & -(\Gamma_{12}+\Gamma_{23}) & \Gamma_{23} \\ \Gamma_{13} & \Gamma_{23} & -(\Gamma_{13}+\Gamma_{23}) \end{pmatrix} \begin{pmatrix} p_1 \\ p_2 \\ p_3 \end{pmatrix}, \tag{1}$$

were $p_{1,\ldots,3}$ describe the populations of the three ground-state sublevels and Γ_{ij} the nuclear-spin relaxation rates for the three possible transitions.

The eigenvalues λ and eigenvectors $\boldsymbol{\xi}$ are thus

$$\lambda_1=0, \quad \lambda_{2\pm}=-(\Gamma_{12}+\Gamma_{13}+\Gamma_{23})\pm r,$$

$$\boldsymbol{\xi}_1=\mathbf{1}, \quad \boldsymbol{\xi}_{2\pm}=\begin{pmatrix} -\Gamma_{12}+\Gamma_{23}\pm r \\ \Gamma_{12}-\Gamma_{13}\mp r \\ \Gamma_{13}-\Gamma_{23} \end{pmatrix}, \tag{2}$$

with

$$r=\sqrt{\Gamma_{12}^2+\Gamma_{13}^2+\Gamma_{23}^2-\Gamma_{12}\Gamma_{13}-\Gamma_{12}\Gamma_{23}-\Gamma_{13}\Gamma_{23}}.$$

The time evolution of the nuclear-spin populations is therefore

$$\boldsymbol{p}(t)=\sum_i a_i \ \boldsymbol{\xi}_i \ e^{\lambda_i t}. \tag{3}$$

The initial nuclear-spin population values $\boldsymbol{p}(t=0)$ depend on the pump configuration: Depending on the ground-state sublevel and to a lesser degree on the excited-state sublevel to which the pump laser couples, it drives the system towards a new quasiequilibrium.[7] Taking into account the different transitions to which the probe laser couples, the absorption change A can be written as

$$A(t,\nu_2-\nu_1)=\sum_{\kappa=1}^{9}\sum_{g,e=1}^{3}|\langle\chi_e|\chi_g\rangle|^2\left(p_{g,\kappa}(t)-\frac{1}{3}\right)L(\Delta\nu). \tag{4}$$

The first sum runs over all pump configurations, while the second sum is over the probe configurations. $|\langle\chi_e|\chi_g\rangle|^2$ is the strength of the transition to which the probe laser couples, ν_1 and ν_2 are the frequencies of the pump- and probe-laser beams, respectively, and $L(\Delta\nu)$ describes the shape of the resonance lines. In the spectra discussed here, it turned out to be well approximated by a Lorentzian.

While the transition strengths are known,[7] Eq. (4) depends on 30 unknown parameters (27 initial spin populations, 3 nuclear-spin relaxation rates), which we wish to determine from the experiment. Since we assume that the sum of the three nuclear ground-state spin populations in each ensemble is constant, 21 independent variables have to be fitted.

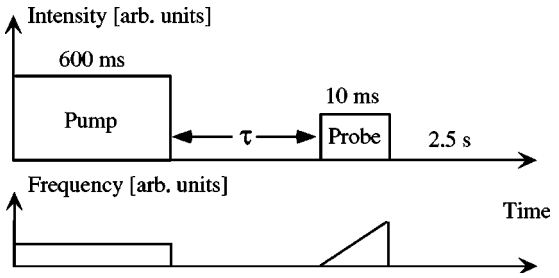

FIG. 4. Timing of the pump and the probe beams. After the pump pulse with a duration of 600 ms and a variable delay τ, the probe beam is turned on for 10 ms and scanned. Between scans probe and pump beams are switched off for 2.5 s, so that the populations can relax to thermal equilibrium.

III. EXPERIMENTAL SETUP

The individual ground-state populations can only be measured if the width of the resonance lines in the hole-burning spectrum is small compared to the separation between them. We therefore had to improve the frequency stability of the dye laser (Coherent 899-21) used for these experiments. We used the Pound Drever scheme[20] to lock our laser to a high finesse confocal Fabry Perot resonator. Under typical operating conditions, this setup reduces the laser jitter to <25 kHz for 1 h.

The pump- and probe-laser beams were derived from the same laser. The frequency of the ring dye laser was set to the center of the inhomogeneous absorption line at 610.7 nm. The two laser beams were shifted independently in frequency with two acousto-optic modulators in a retroreflection setup. These modulators were also used for gating the laser beams. The frequency of the pump beam was fixed while the probe-laser frequency was swept linearly by ± 52 MHz around the pump frequency within 10 ms, using a voltage controlled oscillator.

The experiments were performed on a Pr^{3+}:$YAlO_3$ crystal with the dimensions $5\times5\times1$ mm^3, cooled in a helium flow cryostat at 3–7 K. The pump- and probe-laser beams were both linearly polarized, with a diameter of 1 mm. The pump-laser intensity was 254 W/m^2 and that of the probe laser 64 W/m^2. Since the probe frequency was swept, its effect on the nuclear-spin populations could be neglected, although its intensity was only a factor of 4 smaller than that of the pump laser. The two laser beams propagated along the crystallographic c axis through the sample, intersecting at an angle of 5.7°. Behind the sample, the pump-laser beam was blocked, whereas the probe beam was measured by a photodiode (New Focus 1801).

Figure 4 illustrates the timing of the pump- and probe-laser beams for the time-resolved hole-burning spectra. Under these conditions, the populations of the nuclear-spin states reached a nonthermal equilibrium state within $\approx$600 ms. This was checked by increasing the pump-laser intensity or the pulse duration and verifying that the signal remained unchanged. After the end of the pump pulse, the spin polarization was allowed to decay for a time τ without any laser irradiation before it was measured with a scan of the probe laser. To remove background effects, we subtracted from this signal a dataset that was obtained under otherwise identical conditions, but with the pump laser switched off. After each measurement, both laser beams were switched off for a fixed duration of 2.5 s, so that the system could relax to thermal equilibrium. To increase the signal-to-noise ratio, we averaged over 80 scans.

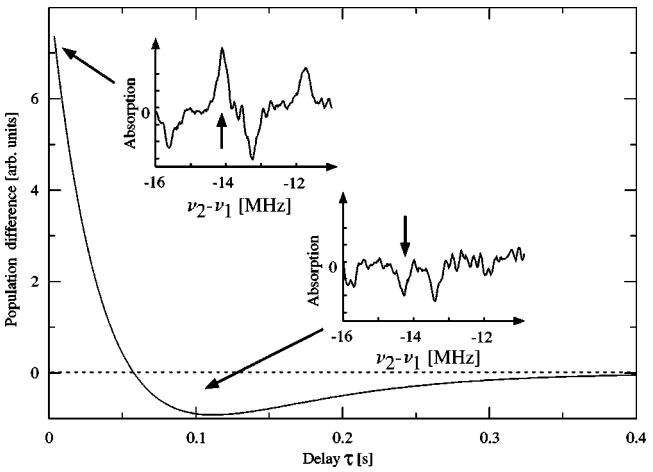

FIG. 5. Calculated decay of the antihole at -14.1 MHz at 5.5 K (full curve) and experimental hole-burning spectra at different times. The nonmonotonic decay is a result of the differences between the relaxation rates. The insets show sections of the experimental hole-burning spectra around -14.1 MHz with positive and negative amplitudes of the antihole.

IV. RESULTS AND DISCUSSION

A. Time dependence

Figure 3 shows for two sections of the hole-burning spectra how the resonance lines decay after the end of the pump pulse. The antiholes of Fig. 3(a) were burned by a pump-laser coupling to the $m=|\pm5/2\rangle$ states of the electronic ground state, while the test laser monitors the ground-state sublevel $m=|\pm1/2\rangle$. The central line at -21.2 MHz arises from those three pump-probe configurations where both lasers couple to the same excited-state sublevel. The other six resonance lines arise from the six remaining pump-probe configurations, each monitoring the decay of a single ground-state sublevel via different probe transitions and starting from different initial conditions.

To determine the rate constants from the time dependence of the spectra, we fitted the amplitude and the offset of each hole and antihole with a Lorenzian curve with constant width, which was derived from the first spectrum ($\tau=0$). Using Eq. (3), we calculated the hole-burning spectra numerically and fitted them to the experimental spectra by adjusting the initial populations $p_{g,\kappa}(0)$ (27 parameters) and the relaxation rates Γ_{ij} (3 parameters).

Figure 5 shows a decay curve measured at a temperature of 5.5 K. The solid curve represents the calculated time dependence of the antihole at -14.1 MHz, using the fitted rate constants $\Gamma_{5/2\leftrightarrow3/2}=10.15$ s^{-1}, $\Gamma_{3/2\leftrightarrow1/2}=5.95$ s^{-1}, and $\Gamma_{5/2\leftrightarrow1/2}=3.09$ s^{-1}. Note that the curve crosses through zero, clearly indicating that the relaxation rates are not equal in

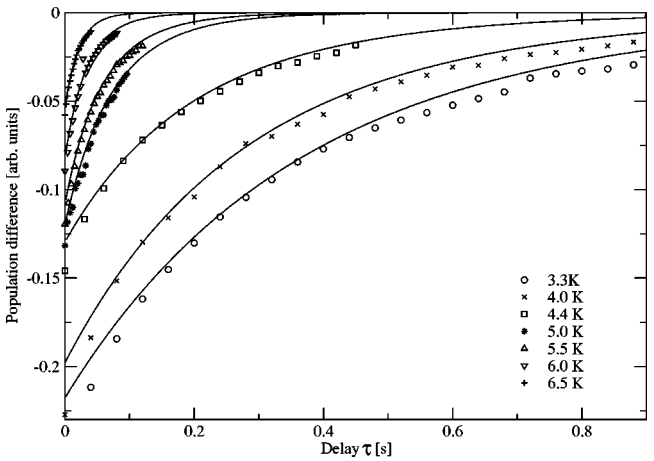

FIG. 6. Decay of the main hole at various temperatures. The solid curve represents the result of the fit.

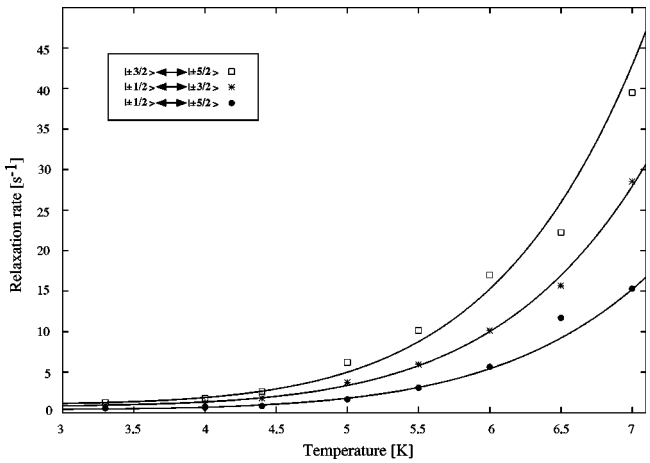

FIG. 7. Nuclear-spin relaxation rates of Pr^{3+}:$YAlO_3$ as a function of temperature. The symbols represent the experimental data points and the solid curves the numerical fit described in the text.

this system. The relevant parts of the experimental hole-burning spectra are also shown for two different delays τ. They clearly show the change from positive to negative amplitude of the peak at -14.1 MHz, indicated by the arrow. The antihole at -14.1 MHz monitors the population of level $|3/2\rangle$. The initial population is $p_3(0)>1/3$. The relaxation of this level is dominated by the fast exchange with level $|5/2\rangle$, which has a population $p_1(0)\ll 1/3$. As a result, the population of level $|3/2\rangle$ becomes smaller than the thermal value for times $\tau>40$ ms and only decays to its equilibrium value on a longer time scale. A similar mechanism can also lead to negative antiholes in the hole-burning spectrum while the pump laser is on. Examples are visible in the inset of Fig. 5 and in the upper trace of Fig. 2 at -15.0, -12.5, and $+12.5$ MHz.

The rate constants found in these measurements are comparable to those found in similar systems,[14,21] but an order of magnitude faster than in Pr^{3+}:LaF_3 at the same doping concentration.[8] We also observe the relaxation between $|\pm 3/2\rangle \leftrightarrow |\pm 5/2\rangle$ to be the fastest, whereas in Pr^{3+}:LaF_3 it is the relaxation between $|\pm 3/2\rangle \leftrightarrow |\pm 1/2\rangle$.

B. Temperature dependence

Since the relaxation rates depend strongly on temperature, we measured the hole-burning spectra over the temperature range of 3.3–7 K. As an example of the temperature dependence, which includes the initial values as well as the rate constants, we show the decay of the main hole at $\nu_1=\nu_2$ for temperatures from 3.3 to 6.5 K in Fig. 6.

Figure 7 summarizes the temperature dependence of the three relaxation rates from 3 to 7 K. The experimental points are fitted with the function

$$\Gamma_{ij}=A_{ij}+B_{ij}T^7, \tag{5}$$

assuming that two distinct relaxation mechanisms dominate in this temperature range: At low temperatures, spin diffusion transports the polarization from the ions that were polarized by the laser to nonresonant ions in their neighborhood. This process is independent of temperature. At higher temperature, thermally activated Raman processes become more important, which typically depend on temperature as T^7–T^9.[22]

The parameters obtained from fitting the temperature dependence are summarized in Table I and are in agreement with earlier measurements with double-resonance techniques.[23] As the relaxation rates increase and the signal-to-noise ratio decreases for higher temperatures, the decay of experimental hole-burning spectra could not be analyzed for temperatures >7 K.

V. CONCLUSION

As we have shown, nuclear-spin relaxation can be measured purely optically, without applying radio frequency fields to the nuclear-spin transitions. The hole-burning spectra used in our experiment require a highly stabilized laser, which can resolve all possible transitions between ground and electronic states.

To analyze the observed decay curves, we used a simple model of the nuclear-spin relaxation, which only takes three

TABLE I. Parameters for the temperature dependence of the nuclear-spin relaxation rates for the electronically ground state $^3H_4$ of Pr^{3+}:$YAlO_3$.

$\|g\rangle \leftrightarrow \|g\rangle$	$A_{ij}(s^{-1})$	$B_{ij}(10^{-5}\ s^{-1}\ K^{-7})$
$\|\pm\frac{1}{2}\rangle \leftrightarrow \|\pm\frac{3}{2}\rangle$	0.79 ± 0.05	3.4 ± 0.1
$\|\pm\frac{1}{2}\rangle \leftrightarrow \|\pm\frac{5}{2}\rangle$	0.39 ± 0.06	1.8 ± 0.1
$\|\pm\frac{3}{2}\rangle \leftrightarrow \|\pm\frac{5}{2}\rangle$	1.0 ± 0.1	5.1 ± 0.3

(double degenerate) states of the electronic ground state into account. This approach gave a satisfactory agreement between the theoretical and experimental hole-burning spectra, although some of the initial amplitudes were off by 10–20 %. These differences may be due to the limitations of the model, which does not include, e.g., the effect of additional electronic states, which participate in the deexcitation process.

The relaxation behavior of the ^{141}Pr nuclear-spin polarization in $YAlO_3$ is similar to the behavior in related systems such as LaF_3.[5,12] At temperatures below 4 K the spin-relaxation behavior was found to be temperature independent. In contrast to Pr^{3+}:LaF_3, where Orbach[24] processes are dominant at higher temperatures, Raman scattering[22] becomes more important in Pr^{3+}:$YAlO_3$ and the relaxation rates increase $\sim T^7$.

The procedure should be generally applicable to systems that produce well-resolved hole-burning spectra. While we have applied this experimental approach to an electronic ground state, it should also be possible to measure relaxation rates in electronically excited states. Compared to the present experiments, a procedure optimized for excited-state measurements would include a shorter preparation time that transports significant population into one of the electronically excited states.

ACKNOWLEDGMENTS

This work was supported by DFG Grant No. Su 192/4–3. The laser stabilization, which was essential for this work, was developed with extensive help from Matt Sellars (ANU Canberra).

*Present address: TOPTICA Photonics AG, Fraunhoferstrasse 14, 82152 Martinsried, Germany.

[1] S. Völker, Annu. Rev. Phys. Chem. **40**, 499 (1989).
[2] M. Mitsunaga, R. Yano, and N. Uesugi, Opt. Lett. **16**, 1890 (1991).
[3] P. Geissinger, L. Kador, and D. Haarer, Phys. Rev. B **53**, 4356 (1996).
[4] L.E. Erickson, Phys. Rev. B **16**, 4731 (1977).
[5] K. Holliday, M. Croci, E. Vauthey, and U.P. Wild, Phys. Rev. B **47**, 14 741 (1993).
[6] R.M. Macfarlane, J. Lumin. **100**, 1 (2002).
[7] R. Klieber, A. Michalowski, and D. Suter, Phys. Rev. B **67**, 184103 (2003).
[8] Y.S. Bai and R. Kachru, Phys. Rev. A **44**, 6990 (1991).
[9] R.G. DeVoe, A. Szabo, S.C. Rand, and R.G. Brewer, Phys. Rev. Lett. **42**, 1560 (1979).
[10] S.C. Rand, A. Wokaun, R.G. DeVoe, and R.G. Brewer, Phys. Rev. Lett. **43**, 1868 (1979).
[11] R.M. Shelby, R.M. Macfarlane, and C.S. Yannoni, Phys. Rev. B **21**, 5004 (1980).
[12] R.G. DeVoe, A. Wokaun, S.C. Rand, and R.G. Brewer, Phys. Rev. B **23**, 3125 (1981).
[13] V.S. Grechishkin and E.M. Shishkin, Fiz. Tverd. Tela (Leningrad) **11**, 893 (1969) [Sov. Phys. Solid State **11**, 730 (1969)].
[14] T. Blasberg and D. Suter, J. Lumin. **65**, 199 (1995).
[15] M.A. Teplov, Zh. Eksp. Teor. Fiz. **53**, 1510 (1967) [Sov. Phys. JETP **26**, 872 (1968)].
[16] M.H. Cohen and F. Reif, Solid State Phys. **5**, 321 (1957).
[17] S. Hüfner, *Optical Spectra of Transparent Rare Earth Compounds* (Academic Press, New York, 1978).
[18] M. Mitsunaga, N. Uesugi, and K. Sugiyama, Opt. Lett. **18**, 1256 (1993).
[19] R.M. MacFarlane and R.M. Shelby, in *Spectroscopy of Solids Containing Rare Earth Ions*, edited by A. Kaplyanskii and R.M. MacFarlane (North-Holland, Amsterdam, 1987).
[20] R.W.P. Drever, J.L. Hall, F.V. Kowalski, J. Hough, G.H. Ford, A.J. Munley, and H. Ward, Appl. Phys. B: Photophys. Laser Chem. **B31**, 97 (1983).
[21] M. Weissbluth, *Atoms and Molecules* (Academic Press, San Diego, 1978).
[22] R. Orbach, in *Electron Paramagnetic Resonance*, edited by S. Geschwind (Plenum, New York, 1972).
[23] T. Blasberg and D. Suter, Chem. Phys. Lett. **215**, 668 (1993).
[24] R. Orbach, Proc. R. Soc. London, Ser. A **264**, 458 (1961).